Molecular Characterization of Inflammatory Myofibroblastic Tumors With Frequent *ALK* and *ROS1* Gene Fusions and Rare Novel *RET* Rearrangement

Cristina R. Antonescu, MD, Albert J.H. Suurmeijer, MD,† Lei Zhang, MSc,* Yun-Shao Sung, MSc,* Achim A. Jungbluth, MD,* William D. Travis, MD,* Hikmat Al-Ahmadie, MD,* Christopher D.M. Fletcher, MD,‡ and Rita Alaggio, MD§*

Abstract: Approximately 50% of conventional inflammatory myofibroblastic tumors (IMTs) harbor *ALK* gene rearrangement and overexpress ALK. Recently, gene fusions involving other kinases have been implicated in the pathogenesis of IMT, including *ROS1* and in 1 patient *PDGFRB*. However, it remains uncertain whether the emerging genotypes correlate with clinicopathologic characteristics of IMT. In this study, we expand the molecular investigation of IMT in a large cohort of different clinical presentations and analyze for potential genotype-phenotype associations. Criteria for inclusion in the study were typical morphology and tissue availability for molecular studies. The lack of ALK immunoreactivity was not an excluding factor. As overlapping gene fusions involving actionable kinases are emerging in both IMT and lung cancer, we set out to evaluate abnormalities in *ALK*, *ROS1*, *PDGFRB*, *NTRK1*, and *RET* by fluorescence in situ hybridization. In addition, next-generation paired-end RNA sequencing and FusionSeq algorithm was applied in 4 cases, which identified *EML4-ALK* fusions in 2 cases. Of the 62 IMTs (25 children and 37 adults), 35 (56%) showed *ALK* gene rearrangement. Of note, *EML4-ALK* inversion was noted in 7 (20%) cases, seen mainly in the lung and soft tissue of young children including 2 lesions from newborns. There were 6 (10%) *ROS1*-rearranged IMTs, all except 1 presenting in children, mainly in the lung and intra-abdominally and showed a distinctive fascicular growth of spindle cells with long cell processes, often positive for ROS1 immunohistochemistry. Two of the cases showed *TFG-ROS1* fusions. Interestingly, 1 adult IMT revealed a *RET* gene rearrangement, a previously unreported finding. Our results show that 42/62 (68%) IMTs are characterized by kinase fusions, offering a rationale for targeted therapeutic strategies. Interestingly, 90% of fusion-negative IMTs were seen in adults, whereas >90% of pediatric IMT showed gene rearrangements. *EML4-ALK* inversion and *ROS1* fusions emerge as common fusion abnormalities in IMT, closely recapitulating the pattern seen in lung cancer.

Key Words: inflammatory myofibroblastic tumor, ALK, ROS1, RET, kinase fusions

(*Am J Surg Pathol* 2015;39:957–967)

Inflammatory myofibroblastic tumor (IMT) is a distinctive neoplasm composed of myofibroblastic-type cells intimately associated with a lymphoplasmacytic inflammatory infiltrate. IMTs can occur ubiquitously at any anatomic site but show a predilection for lung, soft tissue, and viscera of children and young adults. On the basis of its potential for local recurrence and rare metastases, IMT is classified as a mesenchymal neoplasm of intermediate biological potential.[1] Approximately half of the IMTs harbor a clonal translocation that activates the anaplastic lymphoma kinase (ALK)-receptor tyrosine kinase gene located at the 2p23 locus.[2] As a result, ALK protein is overexpressed and can be detected at the immunohistochemical (IHC) level, being used as a reliable diagnostic marker for this disease. ALK is a receptor-type protein tyrosine kinase, which is rendered oncogenic either as a result of a gene fusion, such as in anaplastic large cell lymphoma, lung cancer, and IMT, or due to a missense mutation as seen in neuroblastoma and anaplastic thyroid cancer. In IMT, multiple fusion partners to *ALK* have been described, including *TPM3*, *TPM4*, *RANBP2*, *TFG*, etc., which most likely contribute a strong promoter to the fusion transcript.[2–5]

IMTs display a wide morphologic spectrum, ranging from an inflammatory "pseudotumor" with predominant hyalinization and chronic inflammation and only a paucity of lesional spindle cells, to a highly cellular myofibroblastic proliferation and occasionally frankly

From the *Department of Pathology, Memorial Sloan Kettering Cancer Center, New York, NY; ‡Department of Pathology, Brigham and Women's Hospital, Boston, MA; †Department of Pathology, University Medical Center Groningen, University of Groningen, Groningen, Netherlands; and §Department of Pathology, University of Padova, Padova, Italy.

Conflicts of Interest and Source of Funding: Supported in part by: P50 CA 140146-01 (CRA), Cycle for Survival (CRA). The authors have disclosed that they have no significant relationships with, or financial interest in, any commercial companies pertaining to this article.

Correspondence: Cristina R. Antonescu, MD, Department of Pathology, Memorial Sloan Kettering Cancer Center, 1275 York Ave, New York, NY 10065 (e-mail: antonesc@mskcc.org).

Supplemental Digital Content is available for this article. Direct URL citations appear in the printed text and are provided in the HTML and PDF versions of this article on the journal's Website, www.ajsp.com.

Copyright © 2015 Wolters Kluwer Health, Inc. All rights reserved.

Copyright © 2015 Wolters Kluwer Health, Inc. All rights reserved.

sarcomatous neoplasm, lacking significant inflammatory or/and fibromyxoid stromal component. Because of its markedly variable phenotype and lack of objective immunoprofile, the diagnosis of ALK-negative IMTs has been often a diagnosis of exclusion and regarded as a potential waste-basket of different entities, including reactive/inflammatory processes, such as the fibro-inflammatory IgG4-related disease,[6] idiopathic retroperitoneal fibrosis,[7] and, at the other end of the spectrum, the so-called inflammatory fibrosarcoma. Thus the lack of recurrent genetic abnormalities outside the *ALK* gene rearrangements played a significant drawback in accurate classification of these tumors. Furthermore, ALK immunoreactivity, as an expression of *ALK*-based gene fusions, is more prevalent in pediatric IMT compared with the adult counterpart.[3,8,9] However, it remains unclear whether this discrepant prevalence of ALK abnormalities is an intrinsic difference in the biology of IMT between the 2 age groups, or instead is merely a reflection of a wider spectrum of lesions present in adults that are classified under the broad term of IMT, which otherwise have no genetic relationship. Generally, pathologic features of IMT do not correlate well with behavior.[10] However, the epithelioid variant of IMT, which shows distinctive nuclear membrane or perinuclear ALK immunostaining pattern, has been associated with a more aggressive clinical outcome.[11] In a subset of these lesions an *RANBP2-ALK* fusion has been detected by reverse transcription polymerase chain reaction (RT-PCR). Furthermore, until very recently there was limited knowledge about the pathogenesis of the remaining half of IMTs lacking ALK expression. In this regard, in a seminal study using next-generation sequencing, 6 of 9 ALK-negative IMT tumors showed the presence of fusions in either *ALK*, *ROS1*, or *PDGFRB*, suggesting that IMT is largely a kinase fusion–driven neoplasm.[12] The study was initiated by the dramatic response to the ROS1 inhibitor crizotinib in an index case of a treatment-refractory ALK-negative IMT pediatric patient. In this study, we investigate abnormalities of a wide variety of actionable kinases in a large series of pediatric and adult IMT, encompassing a broad range of clinical presentations to further elucidate their pathogenetic mechanisms and potential correlations with morphology.

MATERIALS AND METHODS

Tumor Samples and Patient Information

The pathology files and the personal consultation files of the senior authors (C.R.A., W.D.T., C.D.M.F., R.A.) were searched for the diagnosis of IMT. Slides were rereviewed, and cases were included in the study if showing a typical morphologic appearance. Tumors were evaluated for their morphologic appearance (spindle, epithelioid), degree of nuclear pleomorphism (mild, moderate), amount of inflammatory component (brisk, scarce), and type (myxoid, fibrous) and amount (prominent, scant) of stroma. ALK immunostaining was reviewed in all cases; however, the lack of ALK immunoreactivity was not an excluding factor. All cases were tested with ALK01 (Ventana; ready to use), and 3 cases were additionally tested with D5F3 (Cell Signaling; 1:50). *ROS1*-rearranged IMTs were then tested with ROS1 antibody (Cell Signaling; clone D4D6; 1:25). Immunostains for SMA, desmin, and myogenin were also reviewed in all cases. None of the ALK-negative tumors showing an immunoprofile in keeping with smooth or skeletal muscle differentiation was included in the study. In fact, only 3 pediatric tumors showed desmin positivity in the absence of myogenin reactivity, 2 of them showing *ALK* gene rearrangement and 1 *ROS1* rearrangement. The study was approved by the Institutional Review Board 02-060.

Fluorescence In Situ Hybridization

Fluorescence in situ hybridization (FISH) on interphase nuclei from paraffin-embedded 4-μm-thick sections was performed applying custom probes using bacterial artificial chromosomes (BAC), covering and flanking genes that were identified as potential fusion partners in the RNA-seq experiment. BAC clones were chosen according to UCSC genome browser (http://genome.ucsc.edu) (Supplementary Table 1, Supplemental Digital Content 1, http://links.lww.com/PAS/A266). The BAC clones were obtained from BACPAC sources of Children's Hospital of Oakland Research Institute (CHORI; Oakland, CA) (http://bacpac.chori.org). DNA from individual BACs was isolated according to the manufacturer's instructions, labeled with different fluorochromes in a nick translation reaction, denatured, and hybridized to pretreated slides. Slides were then incubated, washed, and mounted with DAPI in an antifade solution, as previously described.[13] The genomic location of each BAC set was verified by hybridizing them to normal metaphase chromosomes. Two hundred successive nuclei were examined using a Zeiss fluorescence microscope (Zeiss Axioplan, Oberkochen, Germany), controlled by Isis 5 software (Metasystems, Newton, MA). A positive score was interpreted when at least 20% of the nuclei showed a break-apart signal. Nuclei with an incomplete set of signals were omitted from the score. All cases were tested for *ALK* gene rearrangements. Tumors lacking *ALK* gene abnormalities were further investigated by FISH for changes in *ROS1*, *PDGFRB*, *NTRK1*, and *RET*. *ALK*-positive tumors were further investigated by *EML4* abnormalities by FISH, and *ROS1*-rearranged IMT were tested for *TFG* alterations.

RNA Sequencing and Data Analysis by FusionSeq

Four cases were analyzed by RNA sequencing. Total RNA was prepared for RNA sequencing in accordance with the standard Illumina mRNA sample preparation protocol (Illumina). Briefly, mRNA was isolated with oligo(dT) magnetic beads from total RNA (10 μg) extracted from the cases. The mRNA was fragmented by incubation at 94°C for 2.5 minutes in fragmentation buffer (Illumina). To reduce the inclusion of artifactual chimeric transcripts due to random priming

Copyright © 2015 Wolters Kluwer Health, Inc. All rights reserved.

Copyright © 2015 Wolters Kluwer Health, Inc. All rights reserved.

of transcript fragments into the sequencing library because of inefficient A-tailing reactions that lead to self-ligation of blunt-ended template molecules,[14] an additional gel size-selection step was introduced before the adapter ligation step. The adaptor-ligated library was then enriched by PCR for 15 cycles and purified. The library was sized and quantified using the DNA1000 kit (Agilent) on an Agilent 2100 Bioanalyzer according to the manufacturer's instructions. Paired-end RNA sequencing at read lengths of 50 or 51 bp was performed with the HiSeq 2000 (Illumina).

All reads were independently aligned with the CASAVA 1.8 software provided by Illumina against the human genome sequence (hg19) and a splice junction library, simultaneously. The splice junction library was generated by considering all possible junctions between exons of each transcript. We considered the University of California, Santa Cruz (UCSC) Known Genes annotation set[15] to generate this library using RSEQtools, a computational method for processing RNA-seq data.[16] The mapped reads were converted into Mapped Read Format[16] and analyzed with FusionSeq[17] to identify potential fusion transcripts. FusionSeq is a computational method successfully applied to paired-end RNA-seq experiments for the identification of chimeric transcripts.[18–20] Briefly, paired-end reads mapped to different genes are first used to identify potential chimeric candidates. A cascade of filters, each taking into account different sources of noise in RNA-sequencing experiments, was then applied to remove spurious fusion transcript candidates. Once a confident list of fusion candidates was generated, they were ranked with several statistics to prioritize the experimental validation. In these cases, we used the DASPER score (Difference between the observed and Analytically calculated expected SPER): a higher DASPER score indicated a greater likelihood that the fusion candidate was authentic and did not occur randomly.

Reverse Transcription Polymerase Chain Reaction

An aliquot of the RNA extracted above from frozen tissue (Trizol Reagent; Invitrogen, Grand Island, NY) was used to confirm the fusion transcript identified by FusionSeq. RNA quality was determined by eukaryote total RNA nano assay, and cDNA quality was tested for the PGK housekeeping gene (247 bp amplified product). Three micrograms of total RNA was used for cDNA synthesis by the SuperScript III First-Strand Synthesis Kit (Invitrogen, Carlsbad, CA). RT-PCR was performed using the Advantage-2 PCR kit (Clontech, Mountain View, CA) for 30 cycles at a 64.5°C annealing temperature. Primers used were: EML4_exon2: 5′-AAGATCATGTGGCCTCAGTG-3′ and ALK_exon 20: 5′-AGCTTGCTCAGCTTGTACTC-3′, as previously described.[21] Amplified products were purified and sequenced by the Sanger method.

RESULTS

A total of 62 IMTs were selected on the basis of typical morphologic features and World Health Organization pathologic criteria[1] as well as availability of tissue for molecular and IHC studies. An effort was made to include a wide variety of anatomic locations and ages at presentation. Microscopically, the cohort also covered a broad spectrum of morphologies, spanning from a hypocellular proliferation with hyalinized and prominent chronic inflammatory component, reminiscent of the so-called "inflammatory pseudotumor," to a highly cellular spindle or epithelioid neoplasm with minimal inflammation or stroma. As only half of the IMTs reported in the literature show ALK immunoexpression, the lack of ALK staining was not an exclusion criterion in the presence of an otherwise typical histologic appearance.

Among the 62 cases, the most common locations were lung (n = 18), soft tissue (n = 15), bladder (n = 12), and gastrointestinal (GI) tract and liver (n = 10). Less common sites included head and neck (n = 4) and adrenal and cervix (n = 1 each). One patient presented with disseminated lung, bone, and liver disease.

ROS1 Gene Rearrangements Identified in 10% of IMTs Most Often in Children

There were 6 *ROS1*-rearranged IMTs (Table 1), in 2 cases being associated with a *TFG* fusion (Fig. 1). There were 2 female and 4 male patients, with a mean age of 17.6 years (range, 4 to 61 y). The anatomic locations included 2 in the lung, 3 intra-abdominally, and 1 in the esophagus. All except 1 patient were children, with a mean of 9 years (range, 4 to 18). Both *TFG-ROS1* fusion-positive IMTs occurred in young children, an esophageal mass in a 4-year-old boy and a pelvic tumor in a 4-year-old girl. Morphologically, all pediatric tumors were composed of slender spindle cells with distinctive long cell processes arranged in loose fascicles, associated with mild to moderate inflammatory component and a variably fibromyxoid stroma (Fig. 1). The only nonpediatric IMT with *ROS1* gene rearrangement occurred in the omentum of a 61-year-old man and was composed of plump ovoid cells with marked inflammation (IMT3; Fig. 1). All cases lacked significant cytologic atypia and showed low mitotic activity (1/10). All *ROS1*-rearranged IMTs were negative for ALK IHC; in 1 case (IMT2), the tumor was additionally tested with the more sensitive D5F3 ALK antibody, which was also negative. IHC analysis for ROS1 was performed in 4 cases showing diffuse positivity in 2 tumors (Fig. 1), patchy weak staining in 1, and negativity in the remaining case.

Novel RET Rearrangement was Identified in a Pulmonary IMT

The case occurred in a 27-year-old man with a 7.0 cm mass in the right upper lobe of the lung, which was resected. Follow-up imaging 9 months later revealed a new 9.0 cm lesion in the left kidney, which was proved to be metastatic. The patient succumbed to the disease with widespread metastases 7 months later (IMT7; Table 1).

Copyright © 2015 Wolters Kluwer Health, Inc. All rights reserved.

Copyright © 2015 Wolters Kluwer Health, Inc. All rights reserved.

TABLE 1. Clinical, IHC, and FISH Findings in *ROS1* and *RET*-rearranged IMTs

IMT	Age/ Sex	Location	ROS1/TFG/RET FISH Results	Histologic Findings, MF/10 HPF	ROS1 IHC	ALK IHC
1	18/M	Lung	ROS1 pos/TFG neg	Spindle cells, fascicles, no atypia, 1/10	Neg	Neg
2	7/M	Lung	ROS1 pos/TFG neg	Spindle cells, fascicles, no atypia, 1/10	Pos	Neg*
3	61/M	Intra-abdominal	ROS1 pos/TFG neg	Plump ovoid cells with prominent inflammation, 1/10	ND	Neg
4	12/F	Intra-abdominal	ROS1 pos/TFG neg	Spindle cells, tissue culture–like growth, mild atypia, 1/10	ND	Neg
5	4/M	Esophagus	ROS1 pos/TFG pos	Spindle cells, fascicles, no atypia, 1/10	Pos	Neg
6	4/F	Pelvis	ROS1 pos/TFG pos	Spindle cells, fascicles, no atypia, 1/10	Pos	Neg
7	27/M	Lung	RET pos	Spindle cells, "herring-bone" fascicles, mild atypia, 4/10	ND	Pos

*IHC done with 2 ALK antibodies: ALK01 (Ventana; ready to use) and D5F3 (Cell Signaling; 1:50).
F indicates female; M, male; MF/10 HPF, mitotic figures/10 high-power fields; ND, not done; neg, negative; pos, positive.

The histologies from both primary lung and kidney metastases were reviewed and showed a solid pseudosarcomatous growth, with spindle cells arranged in "herring-bone"-type fascicles. The tumor showed spindle cell morphology with mild to moderate nuclear atypia and up to 4 mitotic figures/10 high-power fields (Fig. 2). The tumor showed immunopositivity for ALK (Fig. 2).

EML4-ALK Fusions Occur With Predilection in Lung and Soft Tissue IMTs

There were 35 cases (56%) with *ALK* gene rearrangement. The presence of *ALK* gene rearrangement correlated with positive ALK IHC staining in most cases, although in some cases the pattern of reactivity was patchy and weak. RNA sequencing was performed in 4 cases, 2 of them with *ALK* fusions (IMT8, IMT9) and 2 negative for all the probes tested (IMT46, IMT48). By FusionSeq, both *ALK*-rearranged tumors showed an *EML4-ALK* fusion candidate (Fig. 3). This result was validated by RT-PCR in 1 case (Fig. 3) and by FISH for *EML4-ALK* fusion assay in both cases (Fig. 3). In the 2 remaining cases no fusion candidate was identified. An additional 5 *ALK*-rearranged IMTs were found to have an *EML4* fusion by screening the remaining *ALK*-positive IMTs by FISH (Table 2). The *EML4-ALK* fusion-positive cases occurred in 6 females and 1 male, all except 2 presenting in children, including 2 newborns (range, 0 to 39 y, mean 15 y). Most occurred in the lung (n = 5), with the remaining 2 in soft tissue (arm, omentum). The 2 IMTs presenting in adult patients included a 36-year-old woman (IMT12) with a tracheal lesion and a 39-year-old woman with a lung lesion (IMT14). Morphologically, all 7 *EML4-ALK* fusion-positive IMTs showed spindle cell morphology with low mitotic activity (1 mitotic figure/10 high-power fields), mild to moderate inflammatory component, and fibromyxoid stroma. Two cases had an intermixed rhabdoid component (Fig. 4). Immunohistochemically, all except 1 case was positive for ALK (Table 2).

From the remaining 28 *ALK*-rearranged tumors, 7 occurred in the lung, 6 in the GI tract and liver, 5 in the bladder, 5 intra-abdominally, 3 in the trunk and mediastinum, and 1 in the head and neck soft tissue (Supplementary Table 2, Supplemental Digital Content 1, http://links.lww.com/PAS/A266). One patient presented with disseminated disease, involving lung, liver, and bone. Although most of the *ALK*-rearranged lesions showed relatively typical morphology, with bland spindle cells, low mitotic activity, mild to moderate inflammation, and fibromyxoid stroma, 2 cases showed distinctive epithelioid morphology, with high mitotic activity and focal marked nuclear pleomorphism (Fig. 5). In this group, 3 (10%) cases were negative for ALK, whereas in the remaining 25 cases the presence of *ALK* gene abnormalities correlated with the ALK immunoreactivity.

Kinase Fusion–negative IMTs Occur Predominantly in Adults

The remaining 20 cases lacked FISH abnormalities in all kinases tested, including *PDGFRB*, *NTRK1*, and *LTK* (Supplementary Table 3, Supplemental Digital Content 1, http://links.lww.com/PAS/A266, and see the Discussion section). There were 12 male and 8 female patients, with an age range of 9 to 72 years (mean 40 y). All except 2 patients were adults, ranging in age from 20 to 74 years (mean 43 y). The only 2 pediatric cases occurred in the lung of a 9-year-old and in the adrenal gland of a 15-year-old. The anatomic distribution included bladder (n = 7), lung (n = 3), head and neck (n = 3), GI and liver (n = 3), soft tissue (n = 2), and other sites (cervix and adrenal, n = 1 each). In this group, most tumors (14/20, 70%) were negative for ALK immunoreactivity (Supplementary Table 3, Supplemental Digital Content 1, http://links.lww.com/PAS/A266).

Organ Site–associated Patterns of Kinase Fusions

Most pulmonary IMTs were positive for fusions (15/18 cases, 83%), either *ALK* (12 cases), *ROS1* (2 cases), or *RET* (1 case). Of the 12 *ALK*-rearranged lung IMTs, 5 (42%) showed the *EML4-ALK* fusions. In fact, most *EML4-ALK* fusion-positive IMTs occurred in the lung (5/7 [71%] cases). Less than half (42%) of the

Copyright © 2015 Wolters Kluwer Health, Inc. All rights reserved.

Copyright © 2015 Wolters Kluwer Health, Inc. All rights reserved.

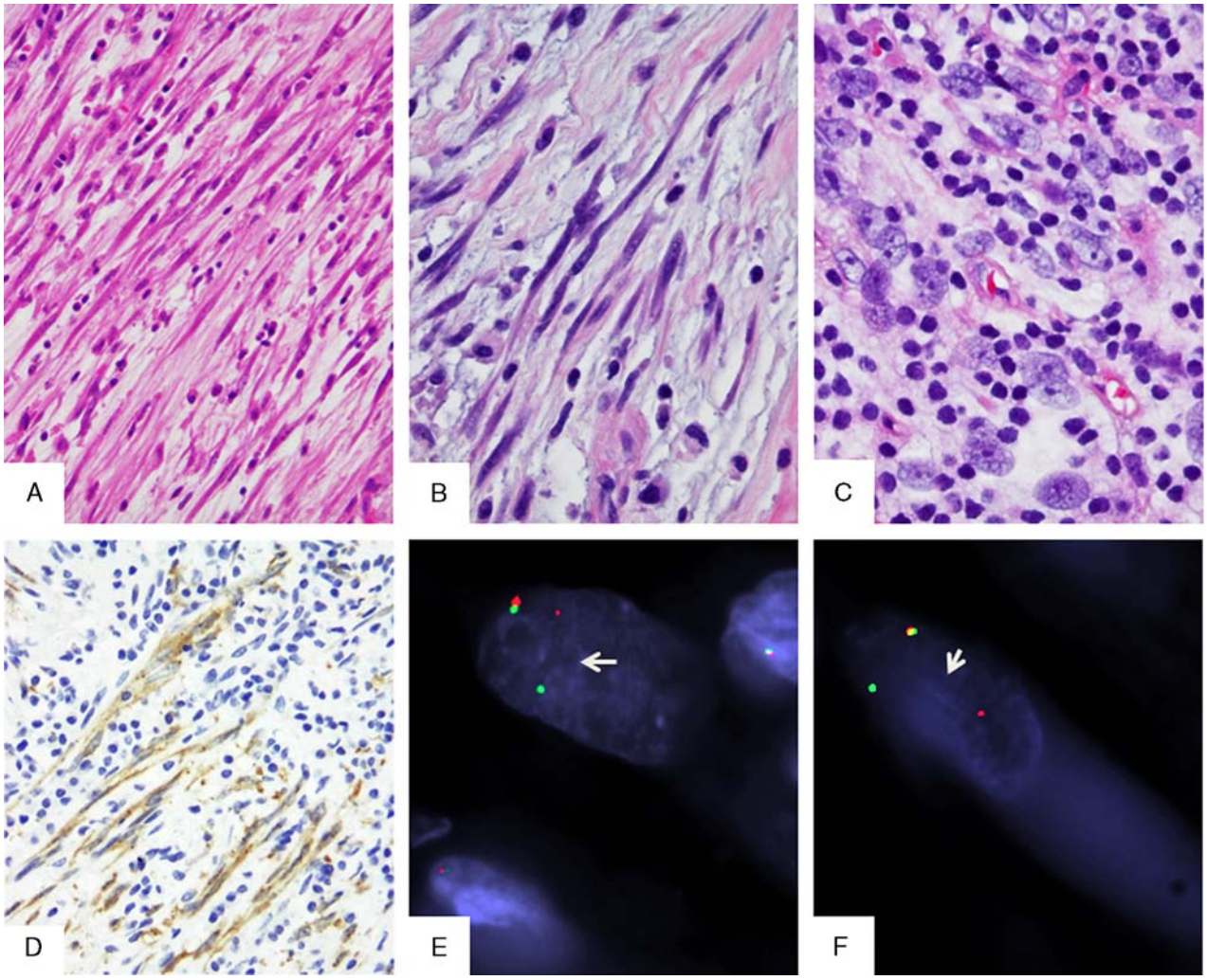

FIGURE 1. Pathologic findings of ROS1-rearranged IMTs. A and B, Most cases showed a distinctive spindle cell proliferation with long, slender cell processes, within a loose edematous stroma with scant inflammatory component (A, IMT6; B, IMT2). C, The only adult IMT case in this genomic group showed more plump cells with ill-defined cell borders, vesicular chromatin and distinctive nucleoli, and more abundant lymphocytic inflammatory infiltrate (IMT3). D, ROS1 immunostaining highlights the long cell processed of lesional cells (IMT2). FISH showing balanced *ROS1* (E) and *TFG* (F) break-apart signals (arrows; IMT6; red, centromeric; green, telomeric).

bladder IMTs showed *ALK* kinase fusions, with most of the cases (83%) being diagnosed in adults.

All except 1 of the head and neck IMTs lacked fusions in any of the kinases investigated, suggesting alternative pathogenesis. Interestingly, most of the fusion-negative IMTs occurred in adults (18/20, 90%), and the prevalent site was the bladder (n = 7). Compared with the *ALK*-rearranged and *ROS1*-rearranged tumors, the fusion-negative IMTs showed an underrepresentation of lung and soft tissue sites and overrepresentation of the head and neck.

DISCUSSION

IMT is currently classified as an intermediate, rarely metastasizing neoplasm composed of myofibroblasts accompanied by an inflammatory infiltrate of plasma cells, variable lymphocytes, and eosinophils.[1] Most patients with IMT are children, adolescents, or young adults, although the tumor can occur throughout life. IMT can occur anywhere in the body, but has a predilection for the abdominal cavity, lung, and bladder.[10,23] Approximately 50% to 70% of the tumors harbor an *ALK* gene rearrangement, leading to the formation of a chimeric fusion protein, which is detectable by IHC or FISH.[2,10] ALK expression and/or *ALK* gene rearrangement was previously described as a good prognostic marker in IMT, with positive cases showing a better outcome, whereas ALK-negative IMTs were more aggressive with a higher frequency of metastasis compared with ALK-positive IMTs.[9,10] However, it is possible that ALK-negative tumors represent either IMT with different genetic abnormalities or different entities altogether.

Copyright © 2015 Wolters Kluwer Health, Inc. All rights reserved.

Copyright © 2015 Wolters Kluwer Health, Inc. All rights reserved.

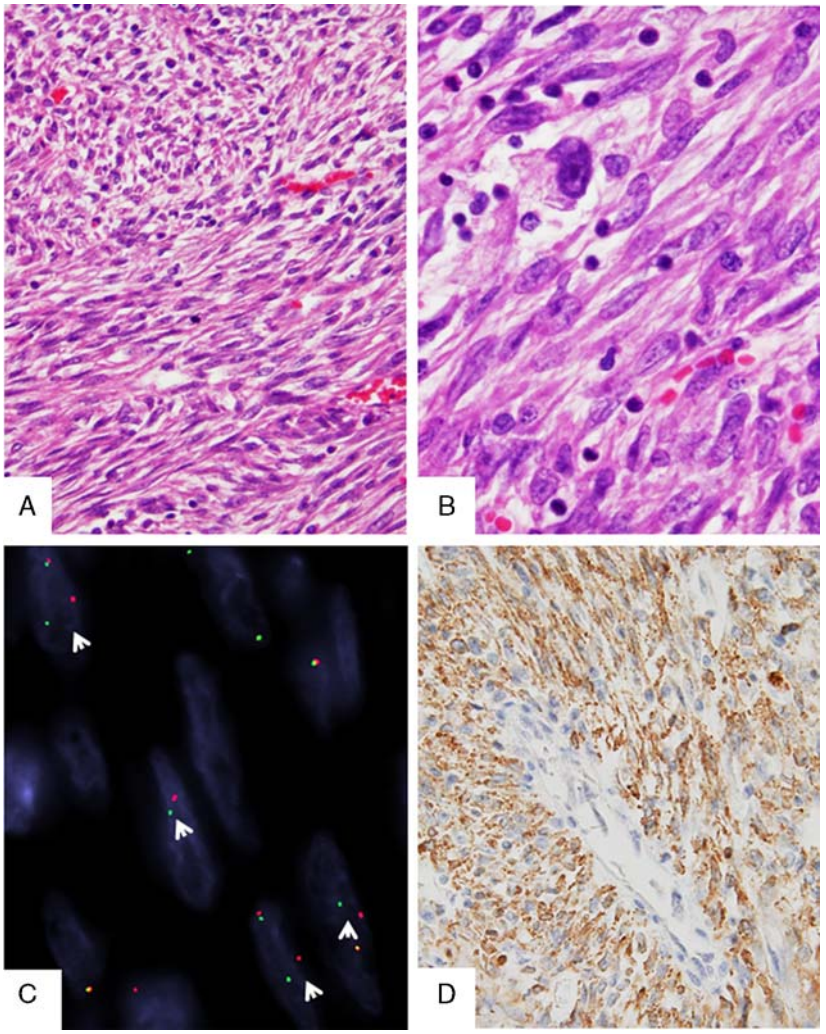

FIGURE 2. Novel RET rearrangement in a pulmonary IMT (IMT7). A and B, A compact proliferation of relatively monotonous spindle cells arranged in intersecting long fascicles, with scant intervening stroma and mild inflammation. Higher power depicts scattered pleomorphic cells with enlarged nuclei and prominent nucleoli. C, FISH assay showing break-apart signals consistent with RET gene rearrangement (arrows; red, centromeric; green, telomeric). D, ALK IHC showing diffuse reactivity.

ALK is a receptor-type protein tyrosine kinase that is currently the focus of much attention in oncology. ALK is rendered oncogenic as a result of its fusion to many gene partners, more commonly to *NPM* in anaplastic large cell lymphoma,[24] to *TPM3* or *TPM4* in IMT,[3] to *EML4* in non–small cell lung carcinoma (NSCLC),[25] and to *VCL* in renal medullary carcinoma.[26–28] It is also activated as a result of missense mutations in neuroblastoma[29] and anaplastic thyroid cancer.[30] The term "ALKoma" was suggested in order to unify these various tumors arising in different organs but sharing oncogenic ALK activation as an essential growth driver, which defines their potential susceptibility to ALK inhibitors.[31] One of such compounds, crizotinib, is now approved in the United States for the treatment of lung cancer positive for *ALK* rearrangement.

ALK fusions similar to other translocations that activate receptor tyrosine kinases bind their catalytic domain to strongly or ubiquitously expressed proteins with dimerization or oligomerization domains. In anaplastic large cell lymphoma, NPM (nucleophosmin) provides both a strong constitutive promoter and an oligomerization domain.[32] Similarly, the TPM3/4 tropomyosin proteins include the coiled coil dimerization domain in the fusion, suggesting a similar role as dimerization partners within these fusions.[3] In IMT, >10 different genes have been identified as *ALK* fusion partners, including *TPM3/4*, *RANBP2*, *TFG*, *CARS*, *ATIC LMNA*, *PRKAR1A*, *CLTC*, *FN1*, *SEC31A*, *EML4*.[12,33] Because of this significant molecular heterogeneity and the fact that most *ALK* gene partners have similar functions in providing a strong promoter and an oligomerization domain, resulting in oncogenic activation of the ALK kinase, our study focused on identifying rearrangements of a large panel of actionable kinases, rather than catalog their ubiquitous partners.

Copyright © 2015 Wolters Kluwer Health, Inc. All rights reserved.

Copyright © 2015 Wolters Kluwer Health, Inc. All rights reserved.

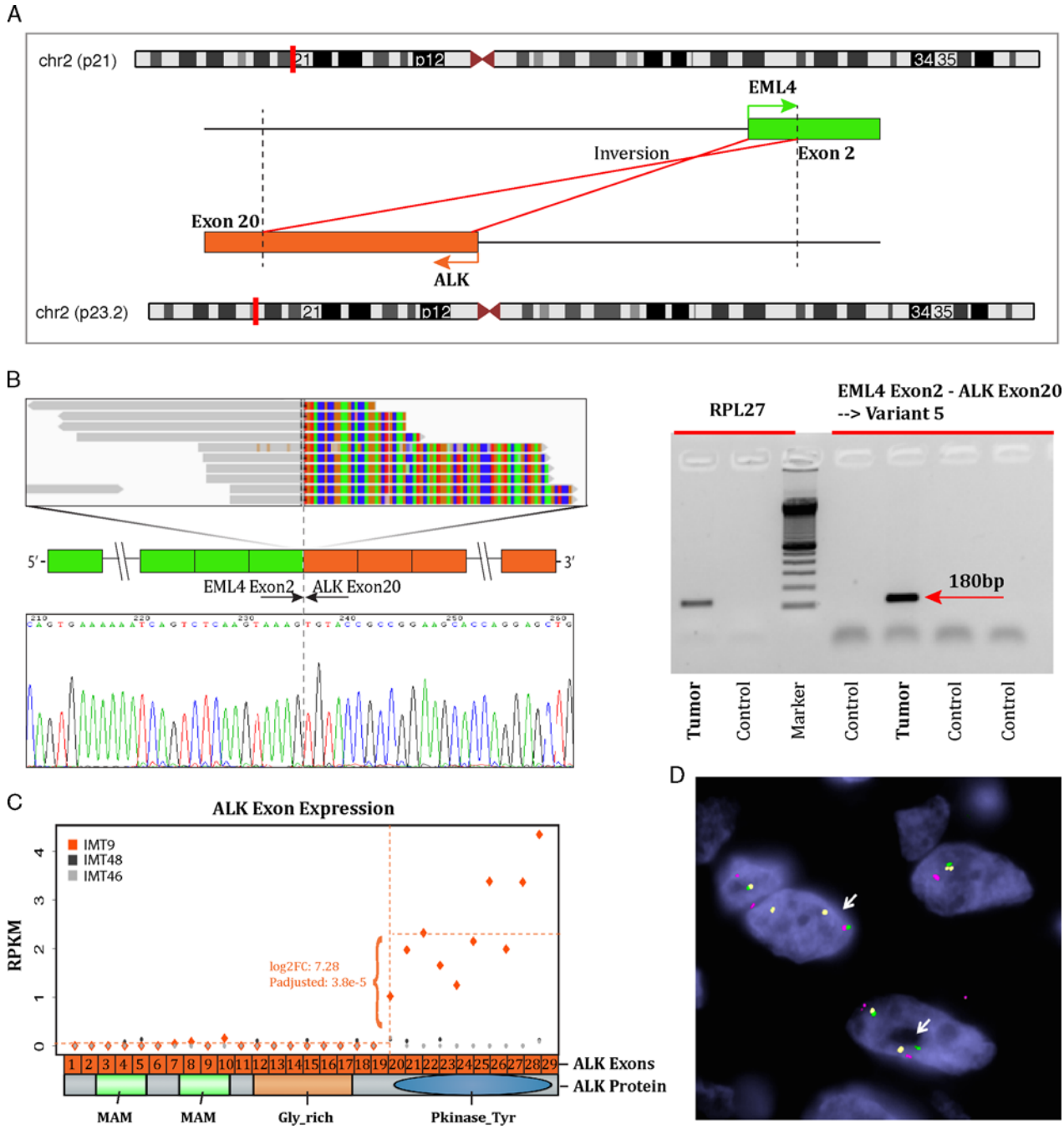

FIGURE 3. RNAseq and FusionSeq discovery of *EML4-ALK* and experimental validation (IMT8-9). A, Schematic representation of the fusion transcript candidate identified by RNAseq, involving the *EML4* locus on 2p21 with *ALK* located on 2p23.2, resulting in an inv2(2)(p21p23) inversion. B, RT-PCR validation and ABI sequence showing that *EML4* exon 2 is fused to *ALK* exon 20, as previously described (IMT8).[22] C, Upregulated expression of the 3′ portion of ALK mRNA starting with exon 20, which is included in the fusion (IMT9). Diagrammatic representation of ALK domains, with the entire kinase domain being preserved in the predicted fusion protein. D, FISH fusion assay showing ALK (red, centromeric) fused to centromeric portion of EML4 (green), away from the telomeric part of EML4, labeled in yellow (IMT9, arrows).

EML4 and *ALK* genes are mapped to the short arm of chromosome 2 in opposite orientations; thus a small inversion inv2(2)(p21p23) is required to give rise to a functional EML4-ALK fusion-type tyrosine kinase.[25] *EML4-ALK* was initially described only in NSCLC; however, a case report recently identified this abnormality in a pulmonary IMT in a 67-year-old man.[34] Subsequently, in the series by Lovly et al,[12] 2 additional

Copyright © 2015 Wolters Kluwer Health, Inc. All rights reserved.

Copyright © 2015 Wolters Kluwer Health, Inc. All rights reserved.

TABLE 2. Clinical and Pathologic Features of *EML4-ALK* Fusion-Positive IMTs

IMT	Age/Sex	Location	Cellular Morphology, MF/HPF	ALK IHC
8*	6 mo/F	Arm	Plump spindle to rhabdoid cells, 1/10	Pos
9*	6/F	Lung	Plump spindle, rare rhabdoid cells, 1/10	Pos
10	5/M	Lung	Spindle cells, 1/10	Pos
11†	NB	Omentum	Spindle cells, 1/10	Pos
12	36/F	Trachea	Spindle cells, 1/10	Pos
13	18/F	Lung	Spindle cells, 1/10	Neg
14	39/F	Lung	Spindle cells, 1/10	Pos

*Confirmed by RNA-seq.
†Dot-like IHC pattern of ALK staining.
F indicates female; M, male; MF/10 HPF, mitotic figures/10 high-power fields; NB, newborn; neg, negative; pos, positive.

EML4-ALK fusion-positive IMTs were identified by RNA-seq, both in the lung. Our study provides further evidence for *EML4-ALK* being involved in the pathogenesis of IMT, which is present in about 20% of the *ALK*-rearranged IMTs studied. We report this gene fusion abnormality in 7 cases, 5 of them occurring in the lung and 2 in the soft tissue, the latter a previously unreported finding. These results suggest that identical *EML4-ALK* present in different tumor types may drive an inappropriate activation of the same kinase signaling pathway, which could be oncogenic in disparate cellular lineages. Both transgenic and CRISPR/Cas murine models expressing EML4-ALK4 in lung epithelial cells were described as resulting in NSCLC phenotype and being responsive to ALK inhibitors.[35,36] None of these genetic models result in an IMT phenotype, suggesting that the transformed cell of origin, that is, lung epithelium, is critical in dictating the phenotype, specifically NSCLC.

ALK receptor tyrosine kinase belongs to the insulin receptor family and is most closely related to leukocyte tyrosine kinase (LTK) with which it shows 79% amino acid identity in the kinase domain and extensive homology elsewhere.[37] As such we have tested the kinase-negative IMT in this series for potential *LTK* gene abnormalities by FISH; however, none was detected, suggesting that this RTK is not involved in the pathogenesis of IMT.

A recent study pointed out that IMTs harbor additional actionable targets, such as *ROS1* and in 1 case *PDGFRB* fusions.[12] This study applying RNA sequencing found that the majority of IMTs (85%) displayed kinase fusions. Notably, *ALK* fusions were detected in 2 of 11 IMT samples that tested negative for ALK expression by

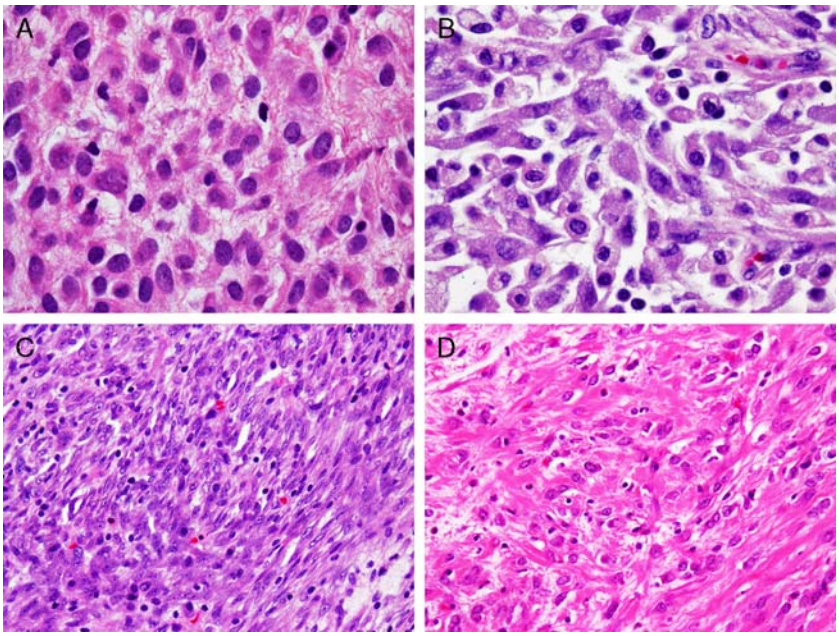

FIGURE 4. Morphologic features of *EML4-ALK* fusion-positive IMTs. A and B, The 2 index cases studied by RNAseq showing epithelioid to rhabdoid-like cells with light eosinophilic to amphophilic cytoplasm, within a loose stroma with scant inflammatory infiltrate (A, IMT8; B, IMT9). The tracheal IMT from a 36-year-old woman (C, IMT12) revealed a compact growth of monotonous spindle cells, whereas the omental IMT from a newborn girl showed a more prominent fibrous stromal component (D, IMT11).

Copyright © 2015 Wolters Kluwer Health, Inc. All rights reserved.

Copyright © 2015 Wolters Kluwer Health, Inc. All rights reserved.

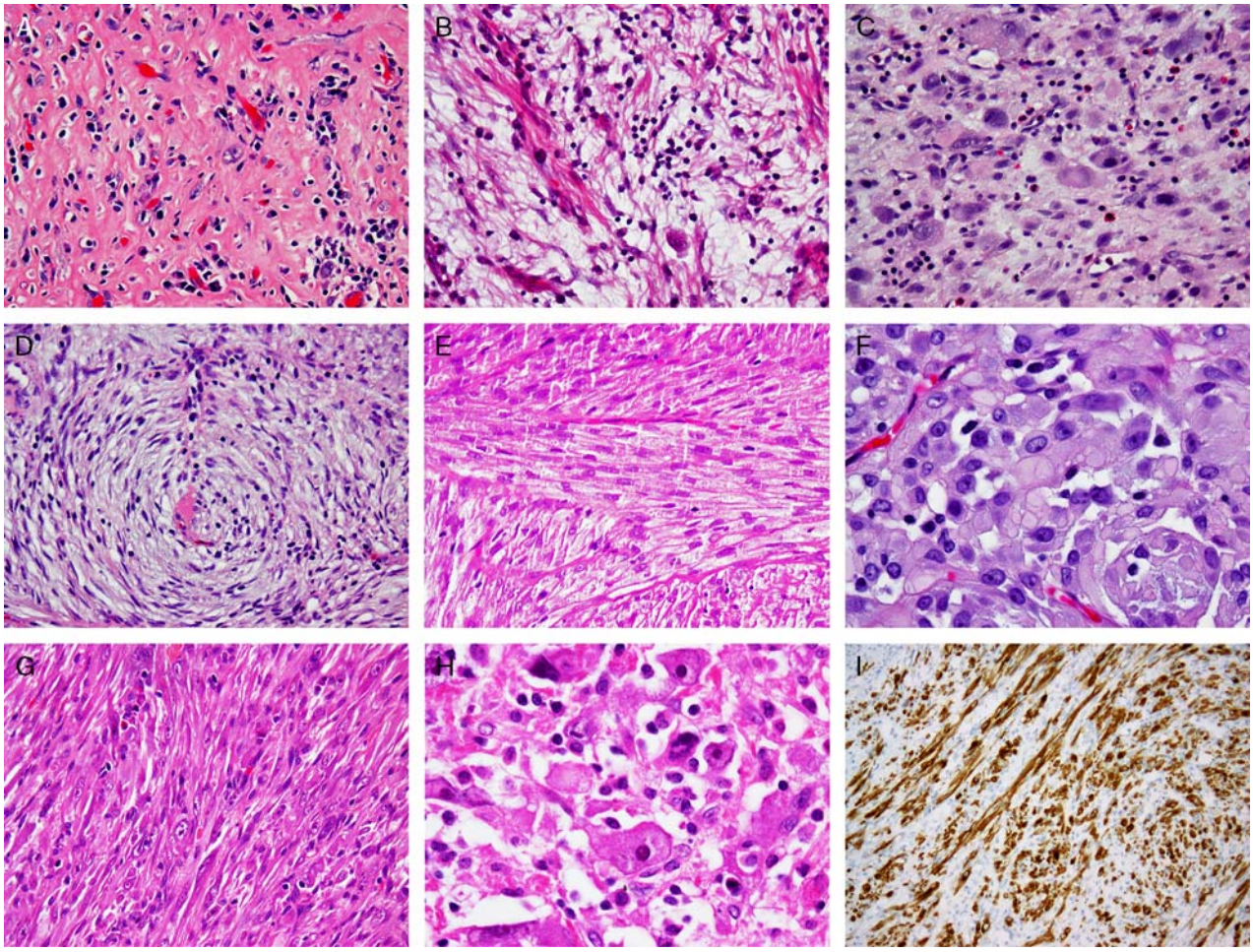

FIGURE 5. Morphologic spectrum of *ALK*-rearranged IMTs. Despite shared ALK gene abnormalities, there was a significant variability in histologic appearance, including: prominent hyalinization and inflammation with only rare lesional cells (A, IMT36); abundant myxoid stroma and moderate degree of inflammation with scattered spindle cells (B, IMT29); enlarged histiocytoid cells separated by conspicuous edematous stroma with numerous eosinophils, reminiscent of Hodgkin lymphoma (C, IMT25); spindle cell morphology with a distinctive whorling pattern and scant inflammation (D, IMT37); solid fascicular growth of monotonous spindle cell with eosinophilic cytoplasm reminiscent of a smooth muscle neoplasm (E, IMT21); distinctive epithelioid morphology, arranged in vague nests (F, IMT39); pseudosarcomatous growth with some cells showing enlarged vesicular nuclei with prominent nucleoli (G, IMT28); pleomorphic phenotype with rhabdoid-like cells showing large open nuclei with virocyte-like inclusions (H, IMT24); strong ALK IHC in a bladder IMT (I, IMT23).

IHC, underlying the risk of denying therapy with an ALK inhibitor on the basis of IHC alone. Our study further emphasizes this caveat, with lack of ALK immunoexpression in 24% (10/42) of fusion-positive IMTs, including all *ROS1*-rearranged cases and 4/35 (11%) *ALK*-rearranged IMTs. It remains to be determined by larger studies whether the more sensitive ALK monoclonal antibody, D5F3, is more reliable in identifying *ALK* gene rearrangements than the ALK01, as they had overlapping results in the 3 cases tested. Similar observations were noted with ROS1 IHC, with only 3 of the 4 *ROS1*-rearranged tumors showing positive staining, including 1 strong and diffuse and the other 2 cases relatively patchy and weak. In our opinion, FISH testing should be performed in IMT with typical morphologic features but negative ALK immunostaining, especially in recurrent/advanced lesions in which systemic therapy with kinase inhibitors could be beneficial.

In the study by Lovly et al,[12] 3 IMT patients with *ROS1*-related fusions are described, involving soft tissue in 2 cases and lung in 1. As *TFG-ROS1* fusions were identified in 2 of the 3 tumors, we have also investigated this specific fusion in our cohort, and found that half of the cases showed similar fusion. Among our 6 *ROS1*-rearranged IMTs, we see a similar anatomic distribution, with 3 in soft tissue, 2 in lung, and 1 in the GI tract (esophagus). In our series, all except 1 tumor occurred in pediatric patients and showed a bland morphologic appearance with spindle cells showing slender and long cell processes.

Our study also describes novel *RET* gene rearrangement in a patient with pulmonary IMT, which

Copyright © 2015 Wolters Kluwer Health, Inc. All rights reserved.

Copyright © 2015 Wolters Kluwer Health, Inc. All rights reserved.

was associated with a fatal clinical outcome. *RET* fusions have been described in NSCLC, typically in younger patients, never-smokers, and in early tumor stages.[22,38] Histologically, *RET* and *ROS1* fusion-positive NSCLCs share the solid signet-ring cell and mucinous cribriform pattern, seen with *ALK* fusion-positive NSCLC.[39] *RET* and *ROS1* fusion-positive NSCLCs comprise about 1% of lung adenocarcinomas, whereas *ALK* rearrangements are seen in 5% of cases.[40]

Despite a comprehensive screening for kinase fusions, studies by both us and Lovly et al[12] identified abnormalities in most but not all IMT cases. In our series, 6/20 (30%) fusion-negative IMTs showed ALK immunoreactivity, suggesting alternative mechanisms of ALK activation. However, most IMTs lacking kinase rearrangements were negative for ALK protein expression, raising the possibility of alternative diagnosis. In the bladder cohort, some of the ALK-negative IMTs with bland morphology could represent postoperative spindle cell nodules or other pseudosarcomatous myofibroblastic proliferations.[41]

In summary, our study investigated genetic abnormalities across a large panel of actionable kinases by combined FISH and RNA sequencing methodology in a diverse clinical and pathologic spectrum of IMTs. As recently reported, our results confirm that two thirds of IMTs show *ALK*-related and *ROS1*-related fusions. Our findings also identify a rare case with novel *RET* gene rearrangement, occurring in a lung IMT. These results further reveal interesting correlations between genotype and clinical presentation in IMT. Most pulmonary IMTs (83%) were positive for fusions, either *ALK* or *ROS1*. In fact, most *EML4-ALK* fusion-positive IMTs (71%) occurred in the lung, with the remaining cases occurring in the soft tissue. Among the 23 pediatric IMTs studied, all expect 2 cases (91%) were positive for kinase fusions, whereas in contrast, most of the fusion-negative IMTs (90%) occurred in adults and rarely arose in lung or soft tissue. These data not only provide insight into this rare tumor type but also offer rational for targeted therapeutic strategies with existing FDA-approved tyrosine kinase inhibitors on the basis of the genomic profile of the tumor.

REFERENCES

1. Fletcher C, Bridge JA, Hogendoorn PC, et al. *WHO Classification of Tumours of Soft Tissue and Bone*. Lyon: IARC; 2013.
2. Griffin CA, Hawkins AL, Dvorak C, et al. Recurrent involvement of 2p23 in inflammatory myofibroblastic tumors. *Cancer Res*. 1999;59:2776–2780.
3. Lawrence B, Perez-Atayde A, Hibbard MK, et al. TPM3-ALK and TPM4-ALK oncogenes in inflammatory myofibroblastic tumors. *Am J Pathol*. 2000;157:377–384.
4. Bridge JA, Kanamori M, Ma Z, et al. Fusion of the ALK gene to the clathrin heavy chain gene, CLTC, in inflammatory myofibroblastic tumor. *Am J Pathol*. 2001;159:411–415.
5. Cools J, Wlodarska I, Somers R, et al. Identification of novel fusion partners of ALK, the anaplastic lymphoma kinase, in anaplastic large-cell lymphoma and inflammatory myofibroblastic tumor. *Genes Chromosomes Cancer*. 2002;34:354–362.
6. Saab ST, Hornick JL, Fletcher CD, et al. IgG4 plasma cells in inflammatory myofibroblastic tumor: inflammatory marker or pathogenic link? *Mod Pathol*. 2011;24:606–612.
7. Vaglio A, Salvarani C, Buzio C. Retroperitoneal fibrosis. *Lancet*. 2006;367:241–251.
8. Coffin CM, Patel A, Perkins S, et al. ALK1 and p80 expression and chromosomal rearrangements involving 2p23 in inflammatory myofibroblastic tumor. *Mod Pathol*. 2001;14:569–576.
9. Chan JK, Cheuk W, Shimizu M. Anaplastic lymphoma kinase expression in inflammatory pseudotumors. *Am J Surg Pathol*. 2001;25:761–768.
10. Coffin CM, Hornick JL, Fletcher CD. Inflammatory myofibroblastic tumor: comparison of clinicopathologic, histologic, and immunohistochemical features including ALK expression in atypical and aggressive cases. *Am J Surg Pathol*. 2007;31:509–520.
11. Marino-Enriquez A, Wang WL, Roy A, et al. Epithelioid inflammatory myofibroblastic sarcoma: An aggressive intra-abdominal variant of inflammatory myofibroblastic tumor with nuclear membrane or perinuclear ALK. *Am J Surg Pathol*. 2011;35:135–144.
12. Lovly CM, Gupta A, Lipson D, et al. Inflammatory myofibroblastic tumors harbor multiple potentially actionable kinase fusions. *Cancer Discov*. 2014;4:889–895.
13. Antonescu CR, Zhang L, Chang NE, et al. EWSR1-POU5F1 fusion in soft tissue myoepithelial tumors. A molecular analysis of sixty-six cases, including soft tissue, bone, and visceral lesions, showing common involvement of the EWSR1 gene. *Genes Chromosomes Cancer*. 2010;49:1114–1124.
14. Quail MA, Kozarewa I, Smith F, et al. A large genome center's improvements to the Illumina sequencing system. *Nat Methods*. 2008;5:1005–1010.
15. Hsu F, Kent WJ, Clawson H, et al. The UCSC known genes. *Bioinformatics*. 2006;22:1036–1046.
16. Habegger L, Sboner A, Gianoulis TA, et al. RSEQtools: a modular framework to analyze RNA-Seq data using compact, anonymized data summaries. *Bioinformatics*. 2011;27:281–283.
17. Sboner A, Habegger L, Pflueger D, et al. FusionSeq: a modular framework for finding gene fusions by analyzing paired-end RNA-sequencing data. *Genome Biol*. 2010;11:R104.
18. Tanas MR, Sboner A, Oliveira AM, et al. Identification of a disease-defining gene fusion in epithelioid hemangioendothelioma. *Sci Transl Med*. 2011;3:98ra82.
19. Pierron G, Tirode F, Lucchesi C, et al. A new subtype of bone sarcoma defined by BCOR-CCNB3 gene fusion. *Nat Genet*. 2012;44:461–466.
20. Mosquera JM, Sboner A, Zhang L, et al. Recurrent NCOA2 gene rearrangements in congenital/infantile spindle cell rhabdomyosarcoma. *Genes Chromosomes Cancer*. 2013;52:538–550.
21. Sanders HR, Li HR, Bruey JM, et al. Exon scanning by reverse transcriptase-polymerase chain reaction for detection of known and novel EML4-ALK fusion variants in non-small cell lung cancer. *Cancer Genet*. 2011;204:45–52.
22. Takeuchi K, Soda M, Togashi Y, et al. RET, ROS1 and ALK fusions in lung cancer. *Nat Med*. 2012;18:378–381.
23. Coffin CM, Watterson J, Priest JR, et al. Extrapulmonary inflammatory myofibroblastic tumor (inflammatory pseudotumor). A clinicopathologic and immunohistochemical study of 84 cases. *Am J Surg Pathol*. 1995;19:859–872.
24. Morris SW, Kirstein MN, Valentine MB, et al. Fusion of a kinase gene, ALK, to a nucleolar protein gene, NPM, in non-Hodgkin's lymphoma. *Science*. 1994;263:1281–1284.
25. Soda M, Choi YL, Enomoto M, et al. Identification of the transforming EML4-ALK fusion gene in non-small-cell lung cancer. *Nature*. 2007;448:561–566.
26. Smith NE, Deyrup AT, Marino-Enriquez A, et al. VCL-ALK renal cell carcinoma in children with sickle-cell trait: the eighth sickle-cell nephropathy?. *Am J Surg Pathol*. 2014;38:858–863.
27. Debelenko LV, Raimondi SC, Daw N, et al. Renal cell carcinoma with novel VCL-ALK fusion: new representative of ALK-associated tumor spectrum. *Mod Pathol*. 2011;24:430–442.
28. Marino-Enriquez A, Ou WB, Weldon CB, et al. ALK rearrangement in sickle cell trait-associated renal medullary carcinoma. *Genes Chromosomes Cancer*. 2011;50:146–153.

Copyright © 2015 Wolters Kluwer Health, Inc. All rights reserved.

Copyright © 2015 Wolters Kluwer Health, Inc. All rights reserved.

29. George RE, Sanda T, Hanna M, et al. Activating mutations in ALK provide a therapeutic target in neuroblastoma. *Nature*. 2008;455:975–978.
30. Murugan AK, Xing M. Anaplastic thyroid cancers harbor novel oncogenic mutations of the ALK gene. *Cancer Res*. 2011;71: 4403–4411.
31. Mano H. ALKoma: a cancer subtype with a shared target. *Cancer Discov*. 2012;2:495–502.
32. Bischof D, Pulford K, Mason DY, et al. Role of the nucleophosmin (NPM) portion of the non-Hodgkin's lymphoma-associated NPM-anaplastic lymphoma kinase fusion protein in oncogenesis. *Mol Cell Biol*. 1997;17:2312–2325.
33. Debelenko LV, Arthur DC, Pack SD, et al. Identification of CARS-ALK fusion in primary and metastatic lesions of an inflammatory myofibroblastic tumor. *Lab Invest*. 2003;83:1255–1265.
34. Sokai A, Enaka M, Sokai R, et al. Pulmonary inflammatory myofibroblastic tumor harboring EML4-ALK fusion gene. *Jpn J Clin Oncol*. 2014;44:93–96.
35. Soda M, Takada S, Takeuchi K, et al. A mouse model for EML4-ALK-positive lung cancer. *Proc Natl Acad Sci USA*. 2008;105:19893–19897.
36. Maddalo D, Manchado E, Concepcion CP, et al. In vivo engineering of oncogenic chromosomal rearrangements with the CRISPR/Cas9 system. *Nature*. 2014;516:423–427.
37. Morris SW, Naeve C, Mathew P, et al. ALK, the chromosome 2 gene locus altered by the t(2;5) in non-Hodgkin's lymphoma, encodes a novel neural receptor tyrosine kinase that is highly related to leukocyte tyrosine kinase (LTK). *Oncogene*. 1997;14: 2175–2188.
38. Kohno T, Ichikawa H, Totoki Y, et al. KIF5B-RET fusions in lung adenocarcinoma. *Nat Med*. 2012;18:375–377.
39. Lee SE, Lee B, Hong M, et al. Comprehensive analysis of RET and ROS1 rearrangement in lung adenocarcinoma. *Mod Pathol*. 2014. [Epub ahead of print].
40. Pan Y, Zhang Y, Li Y, et al. ALK, ROS1 and RET fusions in 1139 lung adenocarcinomas: a comprehensive study of common and fusion pattern-specific clinicopathologic, histologic and cytologic features. *Lung Cancer*. 2014;84:121–126.
41. Hirsch MS, Dal Cin P, Fletcher CD. ALK expression in pseudosarcomatous myofibroblastic proliferations of the genito-urinary tract. *Histopathology*. 2006;48:569–578.

Copyright © 2015 Wolters Kluwer Health, Inc. All rights reserved.

Copyright © 2015 Wolters Kluwer Health, Inc. All rights reserved.